

# Monitoring of biophysical parameters of cashew plants in Cambodia using ALOS/PALSAR data

Ram Avtar · Wataru Takeuchi · Haruo Sawada

Received: 31 August 2011 / Accepted: 10 May 2012 / Published online: 25 May 2012  
© Springer Science+Business Media B.V. 2012

**Abstract** An accurate estimation of a plant's age is required for the prediction of yield and management practices. This study demonstrates the relationship between backscattering properties ( $\sigma^\circ$ ) of Phased Array type L-band Synthetic Aperture Radar (PALSAR) dual polarimetric data with cashew plants' biophysical parameters (height, age, crown diameter, diameter at breast height, basal area, tree density, and biomass) in Cambodia. PALSAR  $\sigma^\circ$  has shown a positive correlation with the biophysical parameters of cashew plants. The value of  $\sigma^\circ$  increases with the age of cashew plants. At a young stage, the cashew plants show a higher rate of an increase in  $\sigma^\circ$  compared to that at the mature stage. The  $\sigma^\circ$  horizontal polarization transmitted and vertical received (HV) shows higher sensitivity to the plant's growth than  $\sigma^\circ$  horizontal polarization transmitted and received (HH). High backscattering and low variations were observed at mature stage (8–12 years) of cashew plantation. Saturation in backscattering has shown from the age of about 13 years. The validation results indicate strong coefficient of determination ( $R^2=0.86$  and  $0.88$ )

for PALSAR-predicted age and biomass of cashew plants with root mean square error=1.8 years and 16.3 t/ha for age and biomass, respectively. The correlations of  $\sigma^\circ$  (HH) with biophysical parameters observed in the dry season were better than those of the rainy season because soil moisture interferes with backscattering in the rainy season. Biomass accumulation rate of cashew plants has been predicted that would be useful for selection of plants species to enhance carbon sequestration. This study provides an insight to use PALSAR for the monitoring of growth stages of plants at the regional level.

**Keywords** Cashew plants' growth · PALSAR · Backscattering coefficient ( $\sigma^\circ$ ) · Plant biophysical parameters · Biomass accumulation rate

## Introduction

Cambodia has 10.09 million ha of forest cover (FRA 2010) and about 10 % (0.9 million ha) is under the concession companies (Economic Land Concession, MAFF, 2010). These concession companies play an important role in the Cambodian economy by managing the forest resources and plantation (Phat et al. 2001). In the recent decades, Cambodia is planting cashew, paulownia, and rubber plants. In Cambodia, about 37,140 ha of total plantation area are covered by cashew plantation (MAFF 2004), and it is increasing year by year. The age of cashew plant is one of the key parameters for

---

R. Avtar (✉) · W. Takeuchi · H. Sawada  
Institute of Industrial Science, The University of Tokyo,  
4-6-1 Komaba, Meguro-Ku,  
Tokyo 153-8505, Japan  
e-mail: ram.envjnu@gmail.com

R. Avtar  
RIGC, Japan Agency for Marine-Earth  
Science and Technology (JAMSTEC),  
Yokohama 236-0001, Japan

estimation of yield, biomass accumulation, and other management practices. Flowering of cashew plant starts from the third year after plantation. It gives a good commercial yield from 5 to 20 years and then shows its reduction (Peter 2007). Therefore, monitoring of the growth of cashew plants can be beneficial in estimating the yield and overall management practices.

Plantation is economically important because it provides incentives in a short period of time (Carle and Holmgren 2008; Lamb 2011). Plantation is also recognized for land rehabilitation, soil conservation, carbon sequestration, water conservation, and provides socioeconomic benefits in minimizing the poverty of local peoples of developing countries (Stephens and Wanger 2007). Therefore, study of biophysical parameters of plants (height, age, crown diameter, diameter at breast height (DBH), basal area, tree density, and biomass) has become necessary for a range of management practices such as determining locations for thinning, harvesting, replantation, yield estimation, and carbon accumulation.

Ground-based characterization of biophysical parameters of plants is a laborious, time-consuming, and expensive task (Trotter et al. 1997; Coops 2002). Therefore, alternative techniques such as remote sensing, comprising of optical and synthetic aperture radar (SAR) systems, are widely used to estimate biophysical parameters of plants on a spatial and temporal scale (Lin and Sarabandi 1999; Wang et al. 2005; Schlerf and Atzberger 2006; Xiao et al. 2006). Conventional optical remote sensing techniques are not effective in tropical countries such as Cambodia because the frequent cloud cover often restrains the acquisition of cloud-free data. On the other hand, optical sensors are usually based on foliage spectral properties, not on the plant's structure (Imhoff et al. 1997; Foody et al. 2003). To overcome these problems, radar remote sensing can be employed in tropical areas for biophysical parameter estimation of plants (Lu 2006; Nizalapur et al. 2010). Various airborne and spaceborne SAR systems with single and multipolarization properties have been widely used in various researches of ecosystem and environment (Ulaby et al. 1982; Le Toan et al. 1992; Ranson and Sun 1994; Dobson et al. 1995; Paloscia et al. 1999; Macelloni et al. 2001; Kasischke et al. 2009).

Biophysical parameters of plants have a significant relationship with the radar backscatter (Coops 2002; Drezet and Quegan 2007). Most of the studies

conducted for the monitoring of plant growth used optical satellite measurements (Ahren et al. 1991; Cohen et al. 1995), which observe surface of the canopy, whereas SAR provides the physical state of plant because of the penetration capability of microwaves (Lavalle et al. 2008). The order of penetration capability depends on the wavelength of the microwaves (Mougin et al. 1999; Jensen 2000). The longer wavelength microwave has high penetration into the canopy. Backscattering coefficient ( $\sigma^\circ$ ) of the SAR is the function of the properties of radar (e.g., wavelength ( $\lambda$ ), polarization, and incident angle ( $\theta$ )) and targets (e.g., soil moisture, surface roughness, vegetation structure, water content, and geometry) (Ulaby et al. 1982; Jensen 2000). The  $\sigma^\circ$  is sensitive to shape, dimension, and other biophysical properties of the plant (Paloscia et al. 1999; Macelloni et al. 2001; Avtar et al. 2011a; Avtar et al. 2012).

This study deals with the use of Phased Array type L-band Synthetic Aperture Radar (PALSAR) dual polarimetric data for estimation of biophysical parameters of cashew plants because of high penetration capability of L-band (23.6 cm) SAR. Co-polarized (HH) and cross-polarized (HV) features of the PALSAR is useful for discrimination of types of scattering from the targets. HH signal interacts with similar orientation, for example, the horizontal branches and soil surface, whereas HV signal is related to volumetric scattering (Rignot et al. 1995; Ouarzedine et al. 2009). The objective of this study is to monitor the age of cashew plants and their biomass in Cambodia based on PALSAR  $\sigma^\circ$  in combination with field-based data to form a biomass accumulation map. This information will enable us to monitor changes in plantation area due to management practices and to investigate the multi-temporal behaviors of  $\sigma^\circ$  from cashew plantation area in different seasons to find the suitable season for monitoring biophysical parameters.

## Study area

The study area is situated near Skuon City, in Kampong Cham Province, Cambodia. It is about 85 km from Phnom Penh and lies between 12°2'17" N to 12°6'7" N latitude and 104°59'51" E to 105°4'23" E longitude (Fig. 1). Cambodia is a tropical country with the rainy season from May to October and dry season from November to April. The minimum and

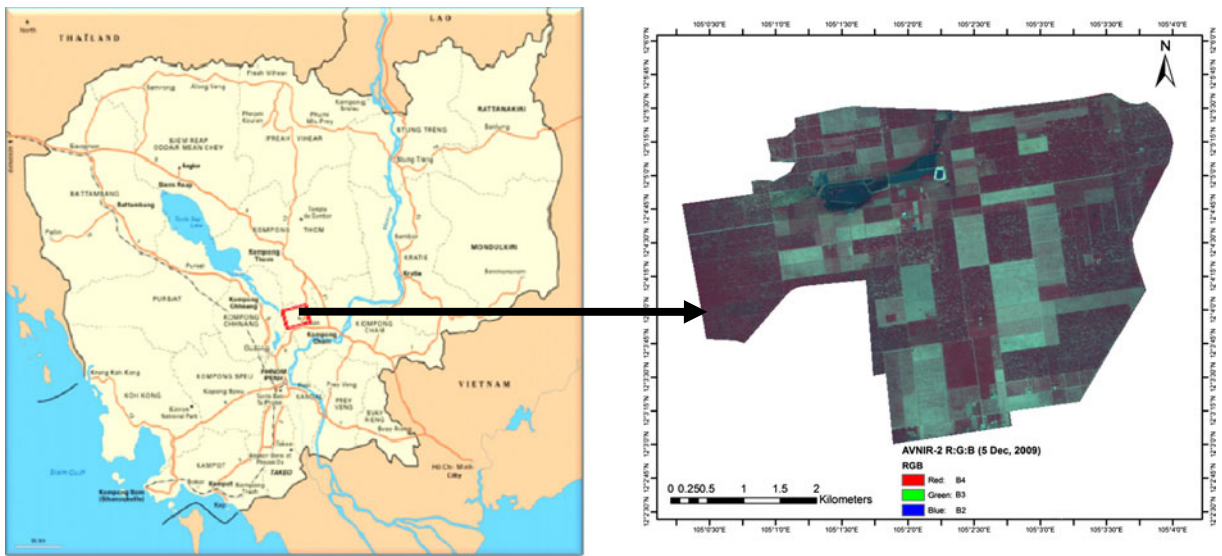


**Fig. 1** Location of the study area

maximum temperature of the study area is about 21 and 35°C, respectively. The mean annual rainfall ranges from 150 to 180 cm (UNEP 2009).

Agrostar private company owns and manages the cashew plantation area of Skuon. Cashew (*Anacardium occidentale*) is an evergreen fast-growing tropical tree that grows up to 10–15 m high with a DBH of 1 m under favorable growing conditions (Rajaona 2008). Cashew is a drought-resistant crop and its ideal temperature is 15 to 35°C. A dry period of 4–6 months with 100–120 cm annual rainfall is ideal for commercial cultivation. These conditions are appropriate in Cambodia for cashew plantation. Cashew plants show three stages of growth: juvenile (1–3 years), young (4–8 years), and mature/old (9–20 years). Cashew plantation area in the study area is on flat plateaus and homogeneously spreads about 2,081 ha, where PALSAR data can be applied for the measurement of biophysical parameters of plants without limitation of topographic effects (based on field survey and ASTER GDEM data analysis).

**Methodology**

**Satellite data used**

Two scenes of dual polarimetric (HH and HV) 1.5 level PALSAR fine beam double polarization (FBD)

data were acquired on 4 September 2010 (rainy season) and 5 December 2010 (dry season) with 34.3° look angle. Landsat ETM + image of 27 December 2010 and Advanced Visible and Near Infrared Radiometer type 2 (AVNIR-2) image of 5 December 2009 were also used to identify the pattern of cashew plantation. Twenty-nine scenes of Landsat images from 1990 to 2010 were also used to establish sampling plots using visual image interpretation to know the trend of cashew plantation activity and history of the starting of cashew plantation. The use of Landsat archive data shows that most of the plantation started in between 1995 and 2000, and it was also confirmed with the results of field-based interviews with the local workers. Hence, satellite archive data show the importance of remote sensing data to know the historical information about land use pattern and changes.

**Field data collection**

Fieldwork was conducted in November 2010. A total of 22 sampling plots were collected to measure and estimate specific biophysical parameters of cashew plants. The stratified random sampling procedure was applied to assure that the sampling measurements captured all possible age classes of cashew plants across the plantation area. The plots were located and established in the field with the use of global

positioning system (GPS), with plot size of 30×30 m to access the accuracy of PALSAR 12.5×12.5 m pixel. Figure 3b shows the layout design of the sampling plot. In each sampling plot tree density, DBH (at 10 cm and 1.3 m from the ground), height, plantation year, site condition, and crown diameter were measured and summarized in Table 1. Thirteen sampling plot data were also collected for validation of results during January 2011. GPS locations and GPS photos of the plots were also collected during the field visit. The biomass of cashew was calculated using the following allometric equation (Eqs. 1 and 2) (Rajaona 2008).

$$\begin{aligned} &\text{Above ground biomass density(t/ha)} \\ &= \text{VOB} \times \text{WD} \times \text{BEF} \end{aligned} \quad (1)$$

where VOB is the volume over bark (in cubic meter per hectare), WD is wood density=0.41 for the cashew

plant (in tons per cubic meter), and BEF is the biomass expansion factor.

$$\text{Cashew plants' biomass(t/ha)} = 1.398 \times \text{DBH} - 0.097. \quad (2)$$

Correlation matrix among the various biophysical parameters (Table 1) has been derived and summarized in Table 2. Correlation matrix shows that all respective biophysical parameters are well correlated, except tree density, and the reason is discussed in “Results and discussion” section.

#### Data processing

Landsat and AVNIR-2 satellite data were used for the prediction of pattern of cashew plantation. However, it was sometimes difficult to identify changes in cashew area because of the cloud cover. Visual image interpretation techniques have been used to identify the pattern of plantation of cashew plants.

**Table 1** Cashew inventory data

Plot_ID	Tree density (no./ha)	Age (years)	Height (m)	Crown diameter (m)	DBH at 10 cm from ground	DBH at 1.3 m from ground	Biomass (t/ha)
Cashew_1	122.0	15	8.7	11.8	44.2	78.7	114.1
Cashew_2	89.0	16	9.1	11.8	54.5	93.5	115.8
Cashew_3	166.0	4	3.3	6.7	19.4	32.2	41.1
Cashew_4	89.0	8	7.5	9.6	33.9	46.7	55.0
Cashew_5	122.0	16	7.7	10.9	49.8	83.4	127.4
Cashew_6	277.0	2.6	3.7	4.4	12.6	12.6	20.9
Cashew_7	122.0	14	9.3	10.4	53.4	70.4	102.2
Cashew_8	178.0	4	4.1	5.4	18.2	18.2	24.2
Cashew_9	89.0	13	7.2	10.5	45.0	82.0	96.0
Cashew_10	133.0	2	1.6	1.3	5.7	5.7	4.7
Cashew_11	122.0	15	6.8	10.6	40.3	61.9	88.5
Cashew_12	133.0	16	7.6	11.2	42.8	60.3	86.4
Cashew_13	166.0	5	4.2	5.8	17.7	26.3	33.6
Cashew_14	89.0	14	8.5	10.9	46.7	72.6	95.1
Cashew_15	222.0	7	3.3	6.9	16.9	34.1	47.3
Cashew_16	128.0	16	10.0	13.2	44.6	75.3	105.6
Cashew_17	128.0	10	6.9	8.5	32.8	54.7	72.0
Cashew_18	128.0	14	7.8	13.7	59.9	87.4	122.3
Cashew_19	277.0	2.7	1.9	3.3	10.5	10.5	13.7
Cashew_20	192.0	16	8.2	10.3	51.6	83.6	143.0
Cashew_21	122.0	12	9.1	8.5	48.3	63.9	87.6
Cashew_22	277.0	9	5.1	5.6	22.4	27.8	54.1

**Table 2** Pearson's correlation matrix of various biophysical parameters of cashew plants

	Tree density	Age	Height	Crown diameter	DBH at 10 cm from ground	DBH at 1.3 m from ground	Biomass
Tree density	1						
Age	-0.58	1					
Height	-0.65	0.90	1				
Crown diameter	-0.64	0.92	0.90	1			
DBH at 10 cm from ground	-0.65	0.93	0.93	0.92	1		
DBH at 1.3 m from ground	-0.66	0.94	0.90	0.94	0.97	1	
Biomass	-0.53	0.95	0.88	0.91	0.95	0.97	1

PALSAR data were processed and digital number (DN) was converted to the normalized radar cross section (or  $\sigma^{\circ}$ ). Then, all imageries were geo-referenced within a pixel accuracy using ground control points collected during field survey. The backscattering (Eq. 3) coefficient was calculated using the following equation (Shimada et al. 2009):

$$\sigma^{\circ} = 10 \times \log_{10}(DN^2) - 83. \tag{3}$$

The data were filtered by the frost filter with the window size of  $5 \times 5$  to reduce speckle noises. We used frost filter because it gives better result (minimize standard deviation with less change in mean value of the pixels) than other filters. The flowchart of methodology used in this study is illustrated in Fig. 2. Figure 3a indicates RGB color composite of the PALSAR FBD speckle-filtered image with sampling plots of cashew plantations. Figure 4 represents the

**Fig. 2** Flowchart of the methodology

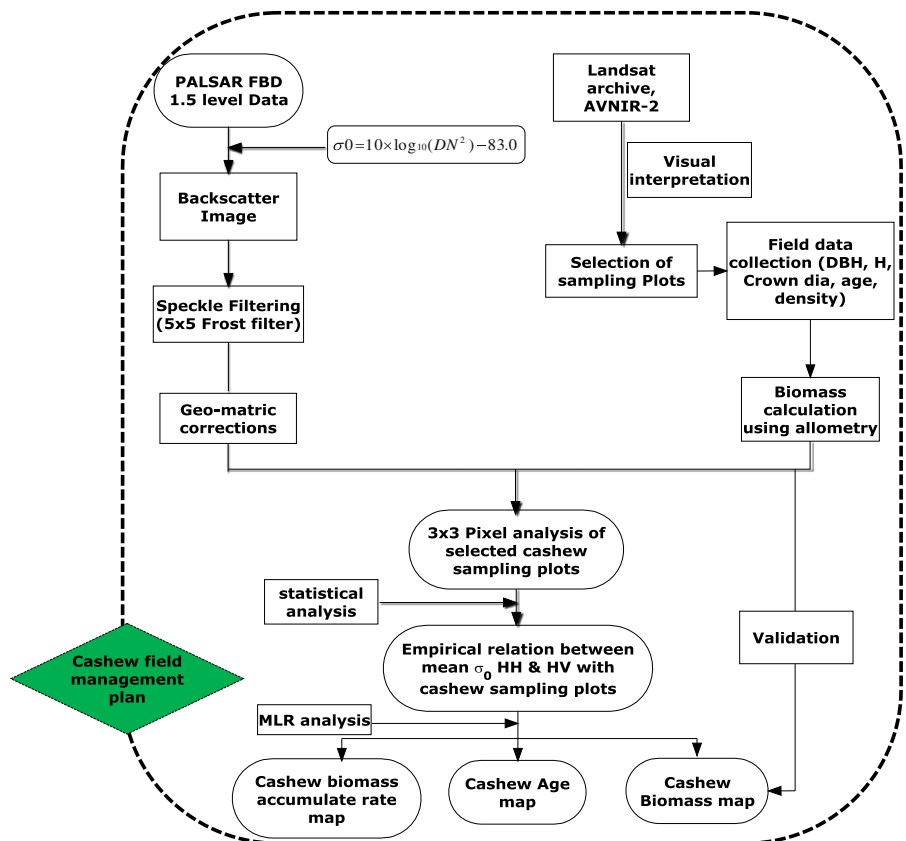


**Fig. 3** **a** PALSAR FBD (5 December 2010) back-scatter image (RGB, HH:HV:HH/HV) with the location of sampling plots in cashew plantation. **b** Layout design of the sampling plot

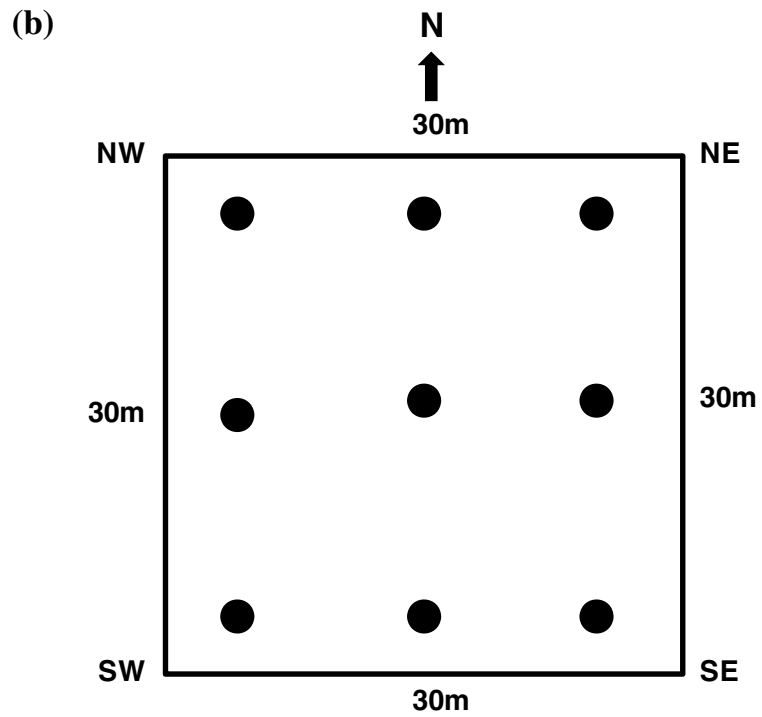
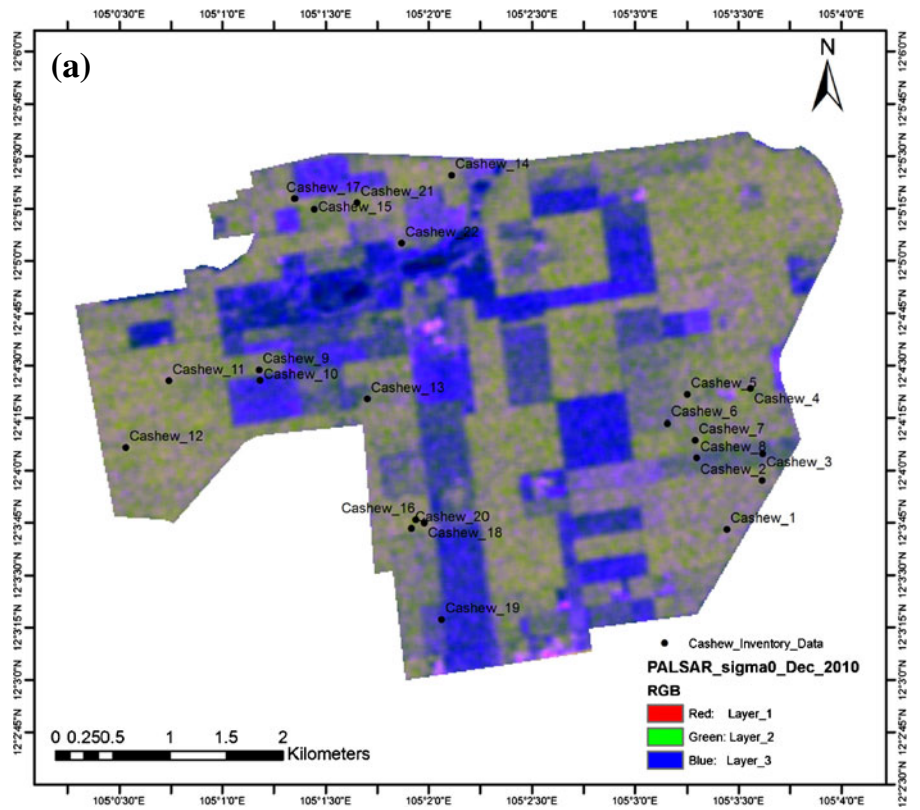


**Fig. 4** Cashew plantation area



snapshot image of the cashew plantation area. This picture shows that the cashew plantation area has a fixed spacing between two plants, and most of the plants have branches at lower than 1 m from the ground. With the growth of cashew plants, the gaps between the canopy decrease, and at mature stage, it shows complete canopy coverage and overlaps with next tree.

In previous studies, researchers widely used radiative transfer model (Eq. 4) to model backscattering coefficient and transmissivity of various targets (McDonald and Ulaby 1993; Dobson et al. 1995). According to Dobson et al. (1995), backscattering behaviors of SAR data depend on the biomass characteristics of plants: (a) in the low biomass area,  $\sigma^\circ$  becomes highly variable, (b) in the moderate biomass area,  $\sigma^\circ$  shows temporal changes because of seasonal change in the canopy and surface properties, and (c) in case of high biomass area,  $\sigma^\circ$  becomes stable because of saturation and very small temporal changes.

$$\sigma^\circ = \sigma_c^\circ + \alpha_c^2 \alpha_t^2 (\sigma_m^\circ + \sigma_t^\circ + \sigma_s^\circ + \sigma_d^\circ) \quad (4)$$

where,

$\sigma^\circ$  is total radar scattering coefficient from woody vegetation

$\sigma_c^\circ$  is backscattering coefficient of the crown layer of smaller woody branches and foliage

$\alpha_c$  is the transmission coefficient of the vegetation canopy

$\alpha_t$  is the transmission coefficient of the trunk layer

$\sigma_m^\circ$  is the multiple-path scattering between the ground and canopy layer

$\sigma_t^\circ$  is the direct scattering from the tree trunks

$\sigma_s^\circ$  is the direct surface backscattering from the ground

$\sigma_d^\circ$  is the double-bounce scattering between the trunks and ground

In this study, analysis of PALSAR backscattering behavior with a  $3 \times 3$  pixel window size was used for different ground-based age classes of cashew plants. We used  $3 \times 3$  pixel window size to minimize positional inaccuracies of GPS and geo-coding. It also minimizes registration problem.

#### Statistical analysis

Correlation analysis has been used to predict the relationship between biophysical parameters of cashew plants and PALSAR  $\sigma^\circ$ . Regression modelling has been adopted because similar plant species exist within the plantation area, except for some area such as water body and recent mango plantation in place of the cashew plants (based on a field survey). Stepwise multi-linear regression analysis (MLR) was used to analyze the relationship between the dependent variable (biophysical parameters) and the independent variables (PALSAR  $\sigma^\circ$  HH and HV). The model was validated by comparing the PALSAR-estimated value with 13 field-based observations collected during January 2011.

#### Results and discussion

Cashew plants' biophysical parameters and their relation with PALSAR  $\sigma^\circ$

Statistical analysis has been done to relate the mean backscatterings of HH and HV polarization with the

biophysical parameters of cashew plantation. Figures 5a–f and Fig. 6a–f show the backscattering of PALSAR dual polarimetry with field-derived biomass, height, crown diameter, DBH, age, and tree density in the dry season (December 2010) and rainy season (September 2010), respectively. Figures 5a–e and 6a–e show high correlation of  $\sigma^\circ$  (HV) with biomass, height, crown diameter, DBH, and age as compared to  $\sigma^\circ$  (HH). The reason why  $\sigma^\circ$  (HV) produces better  $R^2$  than  $\sigma^\circ$  (HH) is because the volumetric

scattering in cashew area enhances the cross-polarization returns (Avtar et al. 2011b). The  $\sigma^\circ$  (HH) is always high because of strong surface scattering. Figures 5f and 6f show a poor correlation ( $R^2=0.21$ ) with tree density due to the decrease in number of trees. The trees are sometimes cut down because of disease and insect damages, mainly at juvenile stage, which ultimately reduce the tree density. Other reason is that the tree density depends on the cashew species and some grafted varieties have high

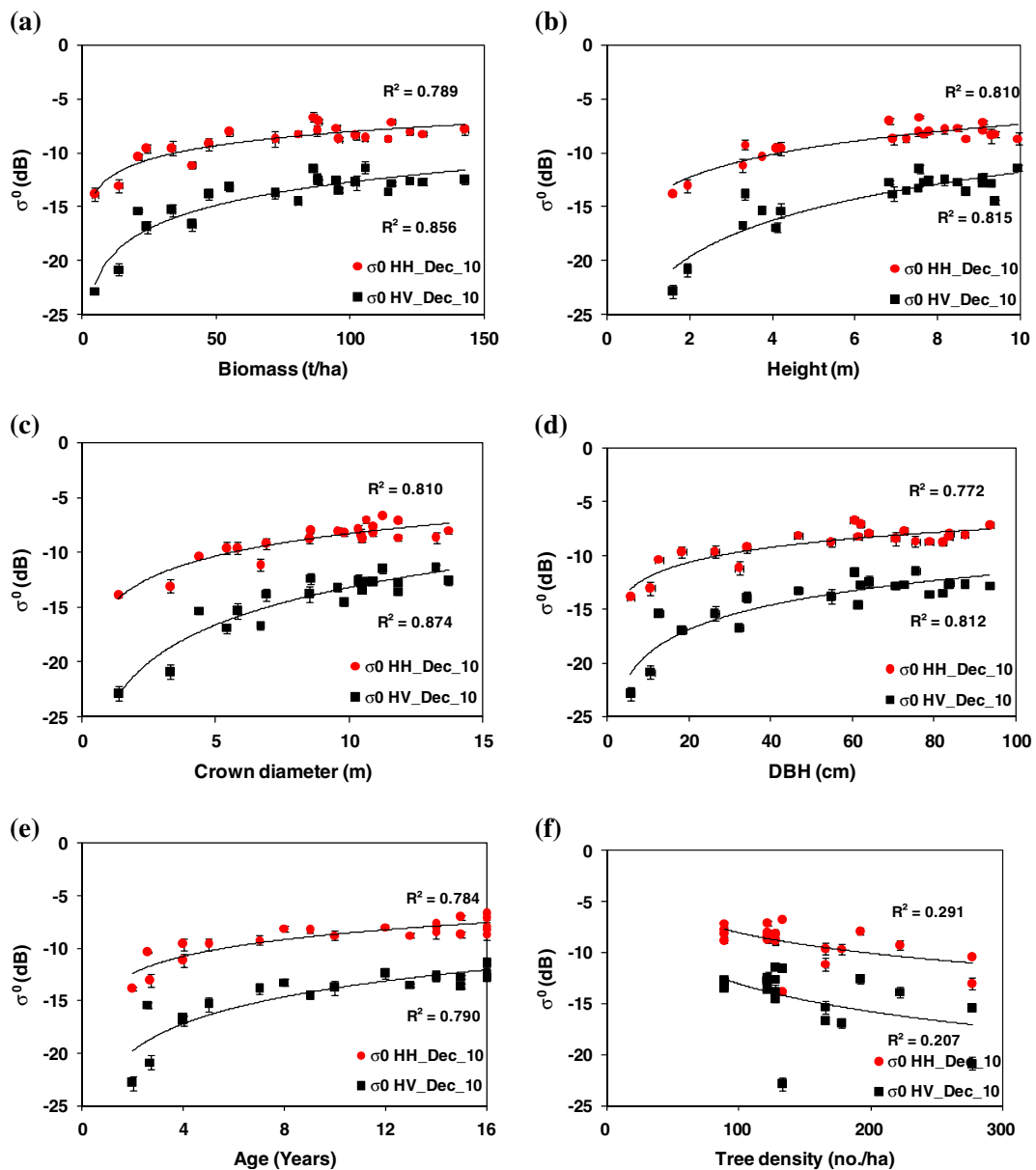


**Fig. 5** Correlation between PALSAR  $\sigma^\circ$  (5 December 2010) and various biophysical parameters of cashew plants' **a** biomass, **b** height, **c** crown diameter, **d** DBH at 1.3 m, **e** age, and **f** tree density

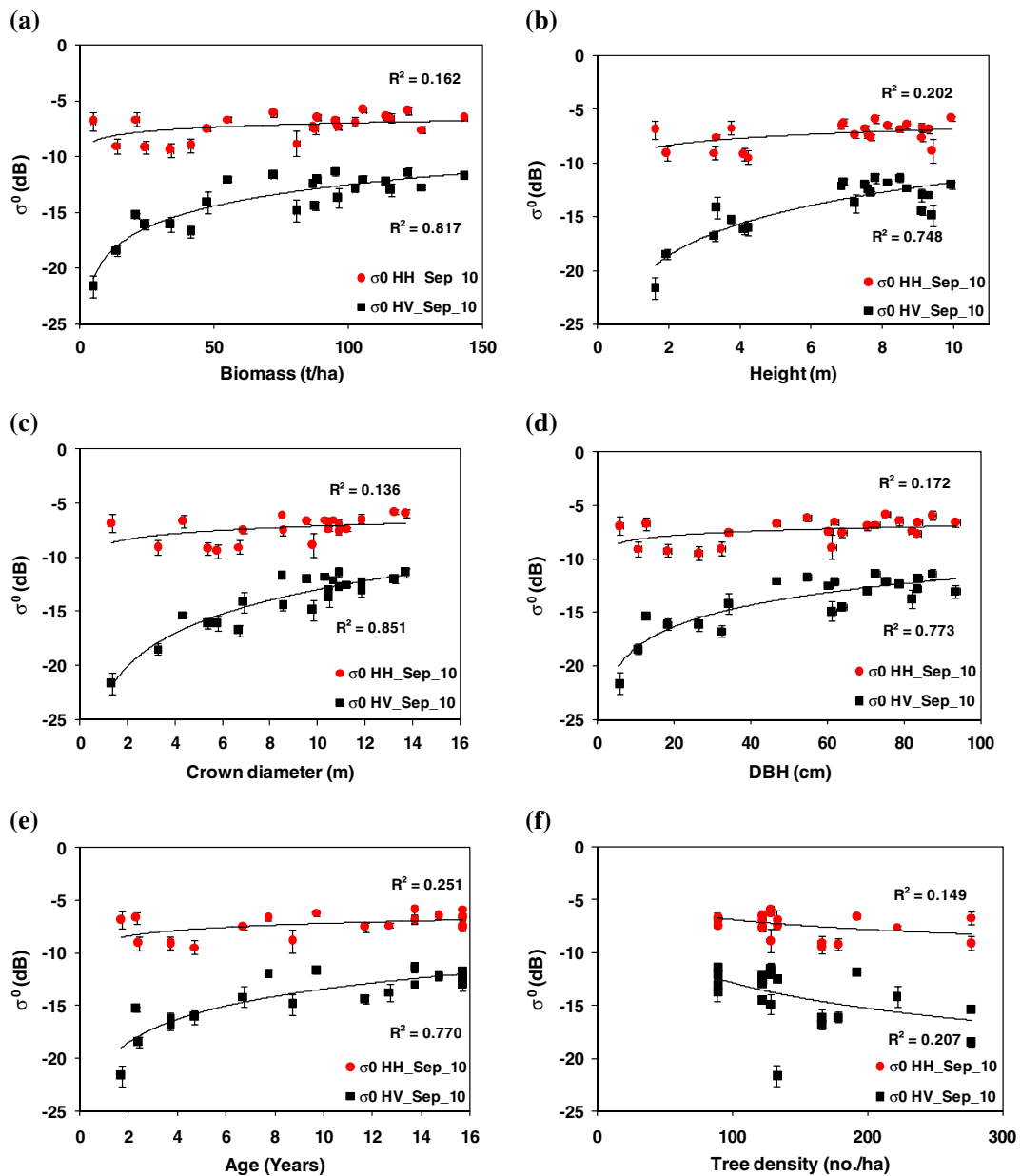


**Fig. 6** Correlation between PALSAR  $\sigma^0$  (4 September 2010) and various biophysical parameters of cashew plants' **a** biomass, **b** height, **c** crown diameter, **d** DBH at 1.3 m, **e** age, and **f** tree density

tree density to get high production (Table 1). Table 1 also illustrates that the tree density is high in young stage, but it becomes low when plants become mature. Because of the above discrepancy, we treated tree density as a conditional parameter. The correlations of  $\sigma^0$  (HH) with biophysical parameters of cashew plants during the dry season were better than those during the rainy season (Table 3). This is mainly because  $\sigma^0$  (HH) is more sensitive to soil moisture

as similar observations were also reported by previous studies using L-band SAR (Le Toan et al. 1992; Dobson et al. 1995; Watanabe et al. 2006; Mitchard et al. 2009).

The relationship between  $\sigma^0$  and cashew plants' age shows that  $\sigma^0$  rapidly increases with the growth of cashew plant. Low backscattering and high variations are seen at juvenile stage (1–3 years) of cashew plants because of variation in surface condition and high

**Table 3** The value of  $R^2$  between cashew biophysical parameters and PALSAR  $\sigma^\circ$  for HH and HV band

	PALSAR FBD 5 December 2010 (dry season)		PALSAR FBD 4 September 2010 (rainy season)	
	$R^2$ ( $\sigma^\circ$ HH)	$R^2$ ( $\sigma^\circ$ HV)	$R^2$ ( $\sigma^\circ$ HH)	$R^2$ ( $\sigma^\circ$ HV)
Biomass	0.79	0.86	0.16	0.82
Height	0.81	0.82	0.2	0.75
Crown diameter	0.81	0.87	0.14	0.85
DBH	0.77	0.81	0.17	0.77
Age	0.78	0.79	0.25	0.77
Tree density	0.29	0.21	0.15	0.21

growth rate during the juvenile stage. After 4 years of growth, the cashew plants become young (Fig. 5a–e). Because of the fast growth, the gaps between the plants decrease considerably within a few years of plantation. At juvenile stage, cashew plants have smaller leaves and fewer branches. This can be a reason why  $\sigma^\circ$  in HH and HV are lower in the juvenile stage. As cashew plant grows, the gaps gradually decrease and the ground surface becomes less visible. As tree crowns increase in size, the importance of the ground attributes diminished and crown attenuation and crown volume scattering increased. High backscattering and low variations are seen at the mature stage (8–12 years) of cashew plant. This increase in  $\sigma^\circ$  is mainly because of growth in biophysical parameters of cashew plants, which indicates structured effects of cashew plants on PALSAR  $\sigma^\circ$ . After a certain growth (15–20 years), the owner starts cutting old cashew plants because of the decline in productivity. Thereby, a decrease of PALSAR  $\sigma^\circ$  at 15 years of age is observed mainly due to disturbances created by cutting older cashew plants. The AVNIR-2 data of December 2009 show that the cashew planted in 1995 has been cut down (Fig. 1). The owner of the area is now planting new grafted cashew plants of high-productive species (based on an interview with local workers). Therefore, this study is useful in providing information about thinning, harvesting, and replantation activity to the owner.

Cashew plants show high branching from the ground level (Fig. 4). It has a large crown diameter overlapping with other trees causing higher volume scattering giving a strong correlation with  $\sigma^\circ$  HV (Figs. 5a–e and 6a–e) compared to  $\sigma^\circ$  HH. Other studies also reveal this fact that  $\sigma^\circ$  HV is more sensitive to biophysical parameters of plants compared to

$\sigma^\circ$  HH (Le Toan et al. 1992; Harrell et al. 1995; Lucas et al. 2006).

Upon comparison of correlations of  $\sigma^\circ$  of PALSAR with the biophysical parameters, we observed a high  $R^2$  for HH and HV in case of the dry season compared to that of the rainy season (Table 3). This is because during the rainy season, the dielectric constant of soil increases due to water which increases backscattering property, as noticed by Dobson et al. (1992), Wang et al. (1994), Schoups et al. (1998), and Kasischke et al. (2009). Result also represents that the effect of soil moisture is more on HH polarization compared to HV polarization.

The  $\sigma^\circ$  of cashew plant shows saturation or decrease in sensitivity after 13 years of growth due to an increase in the biophysical parameters (Figs. 5a–e and 6a–e). Saturation of backscattering coefficient is highly dependent on biophysical parameters of plants as well as characteristics of the radar. Cashew plants show the saturation at 100 t/ha (Fig. 5a); 70 t/ha and 100 t/ha saturation levels of L-band SAR were also noticed by Ruste et al. (1994) and Watanabe et al. (2006), respectively.

#### Cashew plants' biomass, age, and biomass accumulation estimation

Figure 5e shows a clear discrimination between the cashew plants' growth stages and  $\sigma^\circ$  (HH and HV). It increases with the age of cashew plants up to 13 years of cashew growth. MLR model has been generated for cashew age and biomass. Equations 5 and 6 illustrate the MLR model, based on cashew plants' age and biomass (dependent parameters) with  $\sigma^\circ$  HH and HV (independent parameters). This MLR model was applied on PALSAR FBD data of December 2010 to

generate cashew age map (Fig. 7) and cashew biomass map (Fig. 8).

$$Y(\text{age}) = 32.47 + 1.10 \times \sigma^{\circ}\text{HH} + 0.85 \times \sigma^{\circ}\text{HV} \quad (5)$$

$$Y(\text{biomass}) = 237.5 + 4.1 \times \sigma^{\circ}\text{HH} + 8.7 \times \sigma^{\circ}\text{HV} \quad (6)$$

The age map (Fig. 7) shows that most of the area is covered by 11–14-year-old cashew plants. It shows the evidence of cashew plantation between years 1995 and 2000 as investigated from Landsat archive data and field-based interview. The biomass map also shows that most of the area is covered by 76–100 t/ha class of biomass. Biomass value matches with the 11–14-year-old cashew age group, if we compare field-based data (Table 1). Hence, both cashew age and biomass map are well correlated with each other. Figure 9

shows cashew biomass accumulation rate map based on cashew age map (Fig. 7) and biomass map (Fig. 8). The estimated biomass accumulation rate in cashew plants is approximately 7–8  $\text{tha}^{-1} \text{year}^{-1}$ . The biomass accumulation rate of juvenile plants is higher than young and mature plants. This study shows that the cashew plants between 4 and 14 years old accumulate biomass at a relatively constant rate. Accumulation rates in old-aged cashew decrease suddenly because of thinning of the cashew plants. Prediction of biomass accumulation rate has a crucial role in climate change mitigation option. The information about biomass accumulation rate of various plants species can be useful for selection of species having high biomass accumulation rate to enhance carbon sequestration. This study provides the biomass accumulation rate of cashew plants.

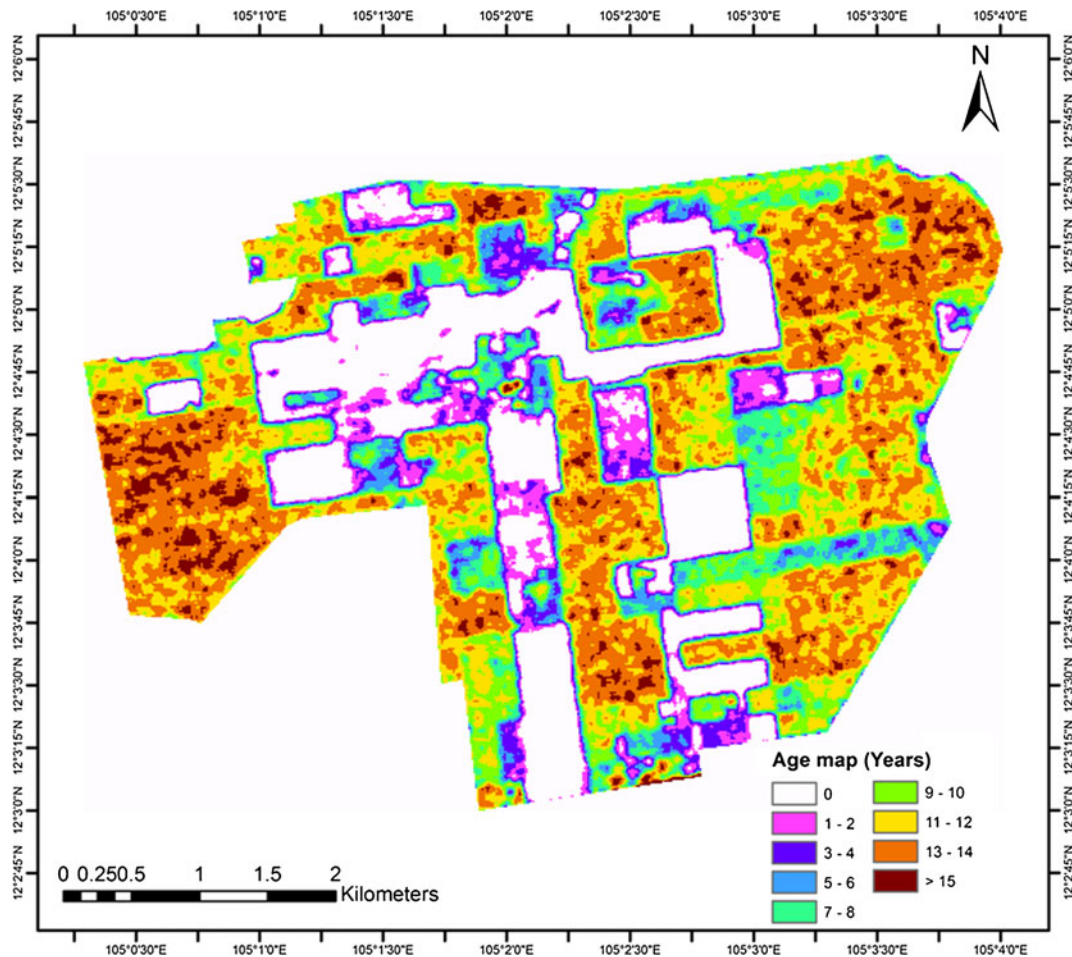
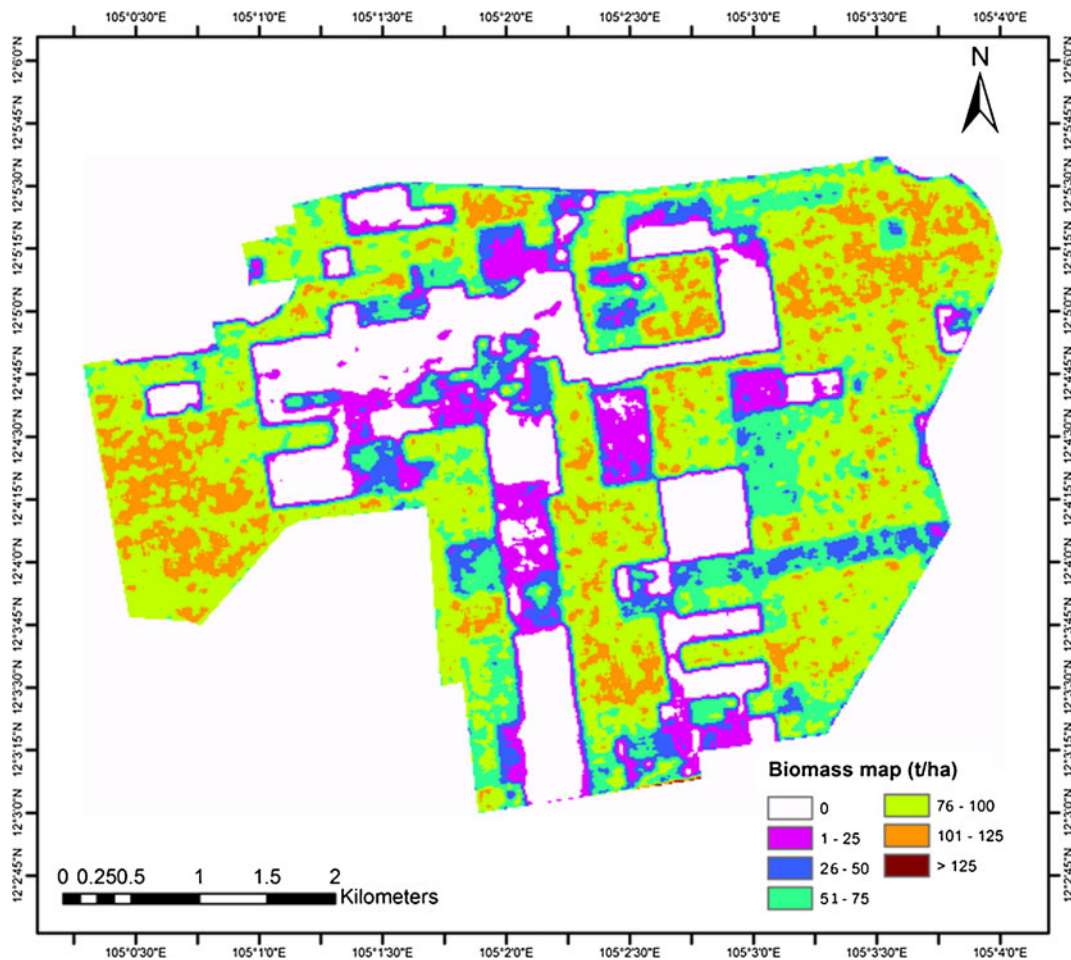


Fig. 7 Cashew age map based on MLR model (PALSAR FBD December 2010 data)



**Fig. 8** Cashew biomass map based on MLR model (PALSAR FBD December 2010 data)

### Validation

Figure 10a shows the validation results of PALSAR-derived cashew plants' age. In general, the graph shows an underestimation of age for juvenile stage because of the same backscattering properties of ground during the early stage of growth (1–2 years). However, it shows a significant coefficient of determination ( $R^2=0.86$ ). The accuracy of the PALSAR-predicted age of cashew plants decreases at the older age after 13 years because of saturation of PALSAR signal. The overall root mean square error (RMSE) for age is 1.8 years and is acceptable to a large extent. The ground truth data of plant age collected during field measurements have an uncertainty of about 1 year because in some cases the local people do not have exact knowledge of the date of plantation. The prediction of age based on PALSAR backscattering will be

useful for estimation of cashew yield because the yield depends on age. This age map can be used by the owner to identify the sites for thinning, harvesting, and replantation. Figure 10b shows the validation results of PALSAR-derived cashew plants' biomass. The accuracy of the PALSAR-predicted age of cashew plants decreases at the high biomass region around 100 t/ha because of saturation of PALSAR signal. The overall RMSE for biomass is 16.3 t/ha. However, the use of multi-sensor remote sensing techniques with the integration of optical, SAR, hyper-spectral, and LiDAR data can provide more precise and accurate information of cashew plants' biophysical parameters. The results obtained from the above regression analysis indicated that the methodology approach adopted in this study could be applicable for the estimation of cashew plants' age, biomass, and biomass accumulation rate.

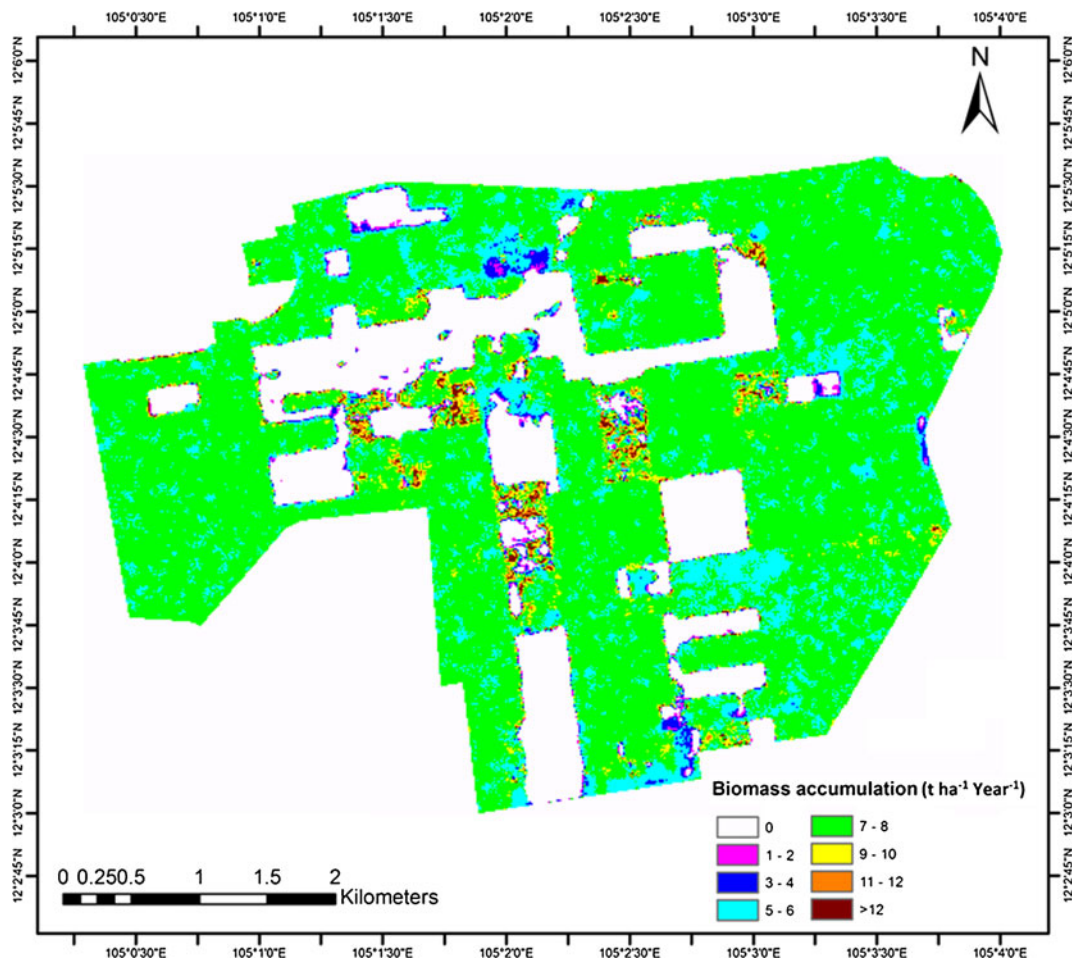


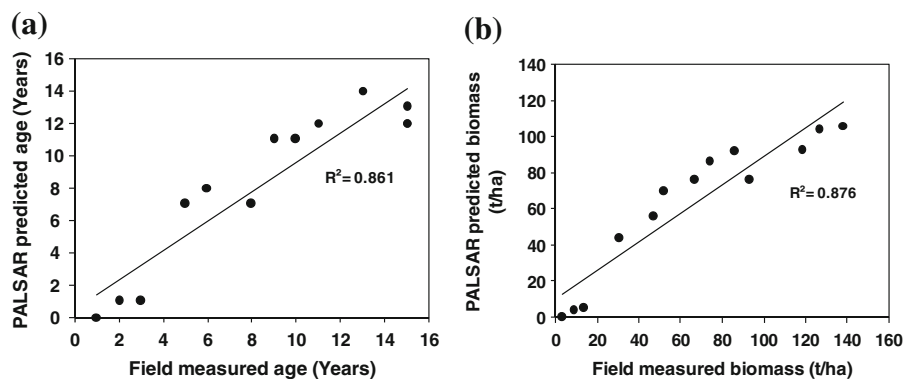
**Fig. 9** Cashew biomass accumulation rate map based on age (Fig. 7) and biomass map (Fig. 8)

**Conclusion**

In conclusion, this study demonstrates the effectiveness of PALSAR FBD data in understanding the relationships between biophysical parameters of cashew

plants and  $\sigma^\circ$ . Statistically significant correlations were found between biophysical parameters of cashew plants and PALSAR  $\sigma^\circ$  except tree density. The back-scattering from HV polarization of PALSAR has shown a strong positive correlation ( $R^2=0.86$  to

**Fig. 10 a** Relationship between PALSAR-predicted cashew age plotted against field-measured age. **b** Relationship between PALSAR-predicted cashew biomass plotted against field-measured biomass (validation)



0.79) with various biophysical parameters of cashew plantation than HH polarization. The correlations of  $\sigma^{\circ}$  (HH) with biophysical parameters observed in the dry season were better than those of the rainy seasons' because soil moisture interferes with backscattering in the rainy season. High backscattering and low variations were observed at mature stage (8–12 years) of cashew plantation. Saturation in backscattering has shown from the age of about 13 years. The validation results indicate strong coefficient of determination ( $R^2=0.86$  and  $0.88$ ) for PALSAR-predicted age and biomass of cashew plants with RMSE=1.8 years and 16.3 t/ha for age and biomass, respectively. The prediction of biomass accumulation rate of cashew plants will also be useful for selection of plant species to enhance carbon sequestration. These results from PALSAR have shown an approach to develop a reliable empirical model for retrieval and monitoring of the biophysical parameters of plants. However, empirical relationships of this study may differ with plant species, types of soil, and environmental conditions. To overcome various limitations, such as saturation of SAR signal, impact of plant species, environmental conditions, etc., we would attempt to use multi-sensor data for further improvement of results.

**Acknowledgments** The authors are highly thankful to the Monbukagakusho (MEXT) Japanese Government Fellowship to pursue research at The University of Tokyo, Japan, and Global Centers of Excellence Program for providing the requisite fund for the field visit. We would like to thank the Forestry Administration, Cambodia for their cooperation during the field data collection. This study was supported by the Environmental Research and Technology Development Fund (F-1101) of the Ministry of Environment, Japan.

## References

- Ahren, F. J., Drdle, T., Maclean, D. A., & Kneppeck, I. D. (1991). A quantitative relationship between forest growth rates and thematic mapper reflectance measurements. *International Journal of Remote Sensing*, *12*, 387–400.
- Avtar, R., Sawada, H., Takeuchi, W., & Singh, G. (2012). Characterization of forests and deforestation in Cambodia using ALOS/PALSAR observation. *Geocarto International*, *27*(2), 119–137.
- Avtar, R., Takeuchi, W., & Sawada, H. (2011a). Full polarimetric PALSAR based land cover monitoring in Cambodia for implementation of REDD policies. *International Journal of Digital Earth*. doi:10.1080/17538947.2011.620639.
- Avtar, R., Takeuchi, W., & Sawada, H. (2011b). Assessment of cashew and rubber plants biophysical parameters based on ALOS/PALSAR data. *Seisan-Kenkyu*, *63*(4), 51–54.
- Carle, J., & Holmgren, P. (2008). Wood from planted forests: a global outlook 2005–2030. *Forest Products Journal*, *58* (12), 6–18.
- Cohen, W. B., Spies, T. A., & Fiorella, M. (1995). Estimating the age and structure of forest in a multi-ownership landscape of western Oregon. *International Journal of Remote Sensing*, *16*, 721–746.
- Coops, N. C. (2002). Eucalypt forest structure and synthetic aperture radar backscatter: a theoretical analysis. *Trees*, *16*, 28–46.
- Dobson, M. C., Ulaby, F. T., Pierce, L. E., Sharik, T. L., Bergen, K. M., Kellndorfer, J., Kendra, J. R., Li, E., Lin, Y. C., Nashashibi, A., Sarabandi, K. L., & Siqueira, P. (1995). Estimation of forest biophysical characteristics in Northern Michigan with SIR-C/X-SAR. *IEEE Transactions on Geoscience and Remote Sensing*, *33*(4), 877–896.
- Dobson, M. C., Ulaby, F. T., Le Toan, T., Beaudoin, A., Kasischke, E. S., & Christensen, N. (1992). Dependence of radar backscatter on coniferous forest biomass. *IEEE Transactions on Geoscience and Remote Sensing*, *30*(2), 412–415.
- Drezet, P. M. L., & Quegan, S. (2007). Satellite-based radar mapping of British forest age and net ecosystem exchange using ERS tandem coherence. *Forest Ecology and Management*, *238*, 65–80.
- Economic Land Concession, MAFF. (2010). <http://www.elc.maff.gov.kh/en/news/12-elc-status.html>
- Foody, G. M., Boyd, D., & Cutler, M. (2003). Predictive relations of tropical forest biomass from Landsat TM data and their transferability between regions. *Remote Sensing of Environment*, *85*(4), 463–474.
- FRA (2010). *Global forest resources assessment. Country reports, Cambodia*, Rome.
- Harrell, P. A., Bourgeau-Chavez, L. L., Kasischke, E. S., French, N. H. F., & Christensen, N. L. (1995). Sensitivity of ERS-1 and JERS-1 radar data to biomass and stand structure in Alaskan boreal forest. *Remote Sensing of Environment*, *54*, 247–253.
- Imhoff, M. L., Sisk, T. D., Milne, A., Morgan, G., & Orr, T. (1997). Remotely sensed indicators of habitat heterogeneity: use of synthetic aperture radar in mapping vegetation structure and bird habitat. *Remote Sensing of Environment*, *60*, 217–227.
- Jensen, J. R. (2000). *Remote sensing of the environmental an earth resource perspective*. Englewood Cliffs: Prentice Hall.
- Kasischke, E. S., Bourgeau-Chavez, L. L., Rober, A. R., Wyatt, K. H., Waddington, J. M., & Turetsky, M. R. (2009). Effects of soil moisture and water depth on ERS SAR backscatter measurements from an Alaskan wetland complex. *Remote Sensing of Environment*, *113*, 1868–1873.
- Lamb, D. (2011). *Regreening the bare hills: tropical forest restoration in the Asia-Pacific region*. New York: Springer.
- Lavalle, M., Solimini, D., & Pottier, E. (2008). PolinSAR for forest biomass retrieval: PALSAR observations and model analysis. *Proceedings of IEEE, IGARSS 2008*, *3*, 302–305.
- Le Toan, T., Beaudoin, A., Riou, J., & Guyon, D. (1992). Relating forest biomass to SAR data. *IEEE Transaction on Geoscience and Remote Sensing*, *30*, 403–411.

- Lin, Y., & Sarabandi, K. (1999). Retrieval of forest parameters using a fractal-based coherent scattering model and a genetic algorithm. *IEEE Transactions on Geoscience and Remote Sensing*, 37(3), 1415–1425.
- Lu, D. (2006). The potential and challenge of remote sensing-based biomass estimation. *International Journal of Remote Sensing*, 27(7), 1297–1328.
- Lucas, R. M., Cronin, N., Lee, A., Moghaddam, M., Witte, C., & Tickle, P. (2006). Empirical relationships between AIRSAR backscatter and LiDAR-derived forest biomass, Queensland, Australia. *Remote Sensing of Environment*, 100, 407–425.
- Macelloni, G., Paloscia, S., Pampaloni, P., Marliani, F., & Gai, M. (2001). The relationship between the backscattering coefficient and the biomass of narrow and broad leaf crops. *IEEE Transactions on Geoscience and Remote Sensing*, 39, 873–884.
- MAFF. (2004). *Agricultural statistics 2003–2004*. Phnom Penh: Ministry of Agriculture, Forestry and Fisheries.
- McDonald, K. C., & Ulaby, F. T. (1993). Radiative transfer modeling of discontinuous tree canopies at microwave frequencies. *International Journal of Remote Sensing*, 14 (11), 2097–2128.
- Mitchard, E. T. A., Saatchi, S. S., Woodhouse, I. H., Nangendo, G., Ribeiro, N. S., Williams, M., Ryan, C. M., Lewis, S. L., Feldpausch, T. R., & Meir, P. (2009). Using satellite radar backscatter to predict above-ground woody biomass: a consistent relationship across four different African landscapes. *Geophysical Research Letters*, 36, L23401. doi:10.1029/2009GL040692.
- Mougin, E., Proisy, C., Marty, G., Fromard, F., Puig, H., Betoulle, J. L., & Rudant, J. P. (1999). Multifrequency and multipolarization radar backscattering from mangrove forestes. *IEEE Transactions on Geoscience and Remote Sensing*, 37(1), 94–102.
- Nizalapur, V., Jha, C. K., & Masugundu, R. (2010). Estimation of above ground biomass in Indian forested area using multi-frequency DLR-ESAR data. *International Journal of Geomatics and Geosciences*, 1(2), 167–179.
- Ouarzedine, M., Souissi, B., & Belhadj-Aissa, A. (2009). *Forest characterization and mapping using fully polarimetric SAR data*. Frascati: PolInSAR 2009.
- Paloscia, S., Macelloni, G., Pampaloni, P., & Sigismondi, S. (1999). The potential of C- and L-band SAR in estimating vegetation biomass: the ERS-1 and JERS-1 experiments. *IEEE Transactions on Geoscience and Remote Sensing*, 37, 2107–2110.
- Peter, K. V. (2007). *Commercial crops technology*. New Delhi: New India Publishing Agency.
- Phat, K., Ouk, N., Uozumi, Y., & Ueki, T. (2001). A case study of the current situation for forest concessions in Cambodia. *Journal of Forest Planning*, 7(2), 59–67.
- Rajaona, A. M. (2008). *Comparative study of allometric parameters of cashew tree (Anacardium occidentale) In North East Brazil*. Master thesis, University of Bonn.
- Ranson, K. J., & Sun, G. (1994). Northern forest classification using temporal multi frequency and multi-polarimetric SAR images. *Remote Sensing of Environment*, 47(2), 142–153.
- Rignot, E. J., Zimmermann, R., & Vanzyl, J. J. (1995). Spaceborne applications of P band imaging radars for measuring forest biomass. *IEEE Transactions on Geoscience and Remote Sensing*, 33(5), 1162–1170.
- Ruste, Y., Hame, T., Pulliainen, J., Heiska, K., & Hallikainen, M. (1994). Radar-based forest biomass estimation. *International Journal of Remote Sensing*, 15, 2797–2808.
- Schlerf, M., & Atzberger, C. (2006). Inversion of a forest reflectance model to estimate structural canopy variables from hyperspectral remote sensing data. *Remote Sensing and Environment*, 100(3), 281–294.
- Schoups, G., Troch, P. A., & Veroest, N. (1998). Soil moisture influences on the radar backscattering of sugar beet fields. *Remote Sensing of Environment*, 65, 184–194.
- Shimada, M., Isoguchi, O., Tadono, T., & Isono, K. (2009). PALSAR polarimetric calibration and geometric calibration. *IEEE Transactions on Geoscience and Remote Sensing*, 47(12), 3915–3932.
- Stephens, S. S., & Wanger, M. R. (2007). Forest plantation and biodiversity: a fresh perspective. *Journal of Forestry*, 105 (6), 307–313.
- Trotter, C. M., Dymond, J. R., & Goulding, C. J. (1997). Estimation of timber volume in a coniferous plantation forest using Landsat TM. *International Journal of Remote Sensing*, 18, 2209–2223.
- Ulaby, F. T., Moore, R. K., Fung, A. K. (1982). *Microwave remote sensing: active and passive*. Volume 2: Radar remote sensing and surface scattering and emission theory, Addison-Wesley, Advanced book program: Reading, Massachusetts, 609.
- UNEP. (2009). *Cambodia environment outlook*. Phnom Penh: Ministry of Environment, Kingdom of Cambodia.
- Wang, Q., Adiku, S., Tenhunen, J., & Granier, A. (2005). On the relationship of NDVI with leaf area index in a deciduous forest site. *Remote Sensing of Environment*, 94(2), 244–255.
- Wang, Y., Kasischke, E. S., Melack, J. M., Davis, F. W., & Christensen, N. L. (1994). The effects of changes in loblolly pine biomass and soil moisture on ERS-1 SAR backscatter. *Remote Sensing of Environment*, 49, 25–31.
- Watanabe, M., Shimada, M., Rosenqvist, A., Tadono, T., Matsuoka, M., Romshoo, A. A., Ohta, K., Furuta, R., Nakamura, K., & Moriyama, T. (2006). Forest structure dependency of the relation between L-band  $\sigma^{\circ}$  and biophysical parameters. *IEEE Transactions on geosciences and remote sensing*, 44(11), 3154–3165.
- Xiao, X. M., Boles, S., Frohling, S., Li, C. S., Babu, J. Y., Salas, W., & Moore, B. (2006). Mapping paddy rice agriculture in South and Southeast Asia using multi-temporal MODIS images. *Remote Sensing of Environment*, 100(1), 95–113.